A stable inversion method for feedforward control of constrained flexible multibody systems

Olivier Brüls[1], Guaraci Jr. Bastos[1], Robert Seifried[2]

[1]Department of Aerospace and Mechanical Engineering (LTAS), University of Liège
Chemin des Chevreuils, 1 (B52/3), 4000 Liège, Belgium

[2]Institute of Engineering and Computational Mechanics, University of Stuttgart
Pfaffenwaldring 9, 70569 Stuttgart, Germany

Abstract

The inverse dynamics of flexible multibody systems is formulated as a two-point boundary value problem for an index-3 differential-algebraic equation (DAE). This DAE represents the equation of motion with kinematic and trajectory constraints. For so-called nonminimum phase systems, the remaining dynamics of the inverse model is unstable. Therefore, boundary conditions are imposed not only at the initial time but also at the final time in order to obtain a bounded solution of the inverse model. The numerical solution strategy is based on a reformulation of the DAE in index-2 form and a multiple shooting algorithm, which is known for its robustness and its ability to solve unstable problems. The paper also describes the time integration and sensitivity analysis methods that are used in each shooting phase. The proposed approach does not require a reformulation of the problem in input-output normal form known from nonlinear control theory. It can deal with serial and parallel kinematic topology, minimum phase and nonminimum phase systems, and rigid and flexible mechanisms.

1 Introduction

High performance machines and robots need to meet conflicting requirements in terms of the weight of the moving masses, the bandwidth of motion and the accuracy of the trajectory. Control schemes based on the assumption of rigid behaviour of the structural components are only valid if the bandwidth of motion is two or three times lower than the first vibration eigenfrequency, which significantly limits the dynamic performance. This motivates the development of control schemes for flexible mechanisms, see, e.g., [1, 2, 3].

Control strategies often combine a feedforward control term, which involves an inverse dynamics model and provides a nominal open-loop control signal, and a feedback control term, which compensates disturbances and uncertainties and stabilizes the system about the nominal trajectory, see Fig. 1. This paper focuses on the feedforward control, which aims at defining the inputs so that the outputs follow a prescribed trajectory. This operation requires the inversion of the open-loop system dynamics and is generally achieved independently of the feedback control. The feedforward control can be computed in a purely algebraic way if the dynamic system is differentially flat [4]. In this case, the system states and inputs can be determined using algebraic relations involving the outputs and a number of their time derivatives, without resorting to any time integration procedure.

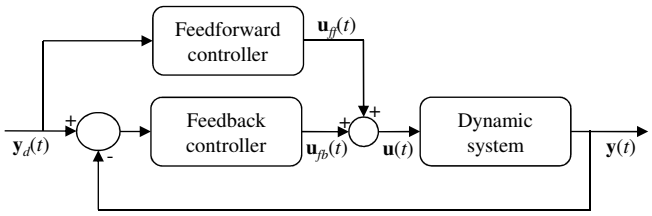

Figure 1: Dynamic system with feedforward and feedback controller

The feedback linearization of robots has been widely studied in the literature; we refer to [5, 6] for a general definition of the feedback linearization concept. This concept is relevant for inverse dynamics problems because any full-state feedback linearizable system is differentially flat [7]. Fully-actuated rigid mechanisms, i.e., mechanisms with the same number of control inputs as degrees of freedom, are feedback linearizable according to the computed torque control technique [8]. As a consequence, they are also differentially flat. In a flexible mechanism, the elastic motion leads to additional degrees of freedom, so the system is underactuated if the number of actuators is still equal to the number of rigid degrees of freedom. If flexibility is only present in the joints, the full state is feedback-linearizable [9] and the system is again differentially flat. If some links are flexible, the system is in general not differentially flat and the inverse dynamics cannot be formulated as a purely algebraic problem.

For non-flat systems, the inverse model consists of an algebraic part and a dynamic part, which is called the internal dynamics in nonlinear control theory [5, 6]. The inverse dynamics problem is usually studied after a reformulation of the dynamics in input-output normal form, so that the internal dynamics explicitly appears as an ordinary differential equation (ODE). This internal dynamics represents the remaining dynamics when the output trajectory is prescribed. For minimum phase systems, the internal dynamics is stable and the inverse dynamics problem can be solved by forward time integration. However, flexible mechanisms are often nonminimum phase [1, 10, 11, 12, 13], which implies that their internal dynamics is unstable and a forward time integration would lead to an unbounded solution, which is of little practical interest. The stable inversion method has been proposed in [14] in order to build a bounded solution to this problem. The first stable inversion method involves a combination of forward and backward time integration of the internal dynamics equation and leads to a non-causal solution. This implies that the control inputs need to start before the beginning of the output trajectory and continue after the end of the trajectory. In [15], the stable inversion problem is reformulated as a two-point boundary value problem for the internal dynamics in ODE form with boundary conditions prescribed at the beginning and at the end of the trajectory. The method is general and has been successfully applied for the control of underactuated and flexible multibody systems [16, 17, 18, 12, 13].

In the aforementioned papers, the stable inversion method requires the reformulation of the equations of the system in input-output normal form, which can be a tedious task in practical applications. Indeed, in multibody dynamics, the equation of motion is often available in the form of a rather complex differential-algebraic equation (DAE). Therefore, this paper investigates a stable inversion algorithm which can deal with the equation of motion in standard DAE form and does not require any symbolic manipulation. A similar strategy was followed in [19, 20], where the inverse dynamics problem is formulated by imposing additional trajectory constraints to the equation of motion. In these two references, the resulting DAE is solved by forward time integration, which is only valid if the system is differentially flat or if the internal dynamics is stable [21]. A more general method, which is also applicable to nonminimum phase systems, is proposed in the present work.

As in [15], the inverse dynamics problem is formulated as a two-point boundary value problem so that a bounded solution can be found even if the internal dynamics is unstable. The present work also contrasts with [22], where the inverse dynamics problem was formulated as a DAE optimal control problem and the objective function was defined to minimize the amplitude of the internal dynamics over the trajectory. Here, the boundary value problem is solved using the multiple shooting method which is known for its robustness, its computational efficiency and its ability to deal with unstable problems [23, 24, 25]. The method is also well-suited for parallelization. The time interval is divided into a number of smaller subintervals and, for each subinterval, the inverse dynamics in DAE form is computed by forward time integration. This integration can be performed even if the internal dynamics is unstable, provided that the shooting subintervals are small enough to avoid a blow-up of the solution.

Among state-of-the-art DAE time integration algorithms, some strategies solve the index-3 problem directly and only rely on the algebraic constraints at position level, while other techniques involve an index reduction and also consider the algebraic constraints at velocity and/or acceleration level. Here, the generalized-α method [26], which is based on the Newmark integration formulas [27], is considered. This method, which is quite popular in structural and flexible multibody dynamics, is well-suited for the solution of stiff problems, which result from the finite element discretization of partial differential equations. The method is proven to be convergent for index-3 DAEs [28]. However, it suffers from spurious numerical oscillations in the transient phase even if the initial values are defined in a consistent way [29]. In the present context, the number of time steps in each shooting subinterval is relatively small, so that these artificial transient oscillations would contaminate a large part of the trajectory. For this reason, a direct integration of the index-3 problem is not recommended. Instead, the reduced-index formulation described in [29] is used. This approach, which is based on the Gear-Gupta-Leimkuhler method [30], is known to be less sensitive to perturbations compared to index-3 methods and it does not exhibit spurious numerical oscillations in the transient phase. The gradient of the final state with respect to the initial state, which is required for the multiple shooting algorithm, is efficiently computed using a semi-analytical direct differentiation method as in [31].

The paper is organized as follows. Section 2 describes the formulation of the inverse dynamics problem as a DAE two-point boundary value problem. The numerical solution method based on a multiple shooting algorithm is presented in Section 3 and the time integration method used in the shooting subintervals is discussed in Section 4. Two examples of flexible manipulators with serial and parallel kinematic topology are studied in Section 5 and some conclusions are drawn in Section 6.

2 Formulation of the Inverse Dynamics Problem

2.1 Equation of motion

Let us consider a flexible multibody system composed of rigid and flexible bodies, joints and force elements. A spatial discretization of the flexible bodies, e.g., using the finite element method, leads to a kinematic description based on n coordinates $\mathbf{q}$, see [32] for a review of formulations. If the coordinates are redundant, they have to satisfy m kinematic constraints, where $n-m$ denotes the number of degrees of freedom of the spatially discretized system. As a consequence, the equation of motion has the structure of a differential-algebraic equation. The system is also actuated by s control inputs which are collected in the $s \times 1$ vector $\mathbf{u}$. Introducing

the $s \times 1$ vector of output variables $\mathbf{y}$, the equation of motion takes the form

$$\begin{aligned} \mathbf{M}(\mathbf{q})\ddot{\mathbf{q}} + \mathbf{g}(\mathbf{q}, \dot{\mathbf{q}}, t) + \mathbf{\Phi}_{\mathbf{q}}^T(\mathbf{q})\,\boldsymbol{\lambda} - \mathbf{A}(\mathbf{q})\,\mathbf{u} &= \mathbf{0} && \text{(1a)} \\ \mathbf{\Phi}(\mathbf{q}) &= \mathbf{0} && \text{(1b)} \\ \mathbf{y} - \mathbf{h}(\mathbf{q}) &= \mathbf{0} && \text{(1c)} \end{aligned}$$

where $\mathbf{M}$ is the mass matrix, $\mathbf{g}$ is the vector of internal, external and complementary inertia forces, $\mathbf{\Phi}$ is the vector of m kinematic constraints, $\boldsymbol{\lambda}$ is the vector of m Lagrange multipliers and $\mathbf{\Phi}_{\mathbf{q}} = \partial\mathbf{\Phi}(\mathbf{q})/\partial\mathbf{q}$ is the matrix of constraint gradients. The input matrix $\mathbf{A}$ distributes the s control inputs $\mathbf{u}$ onto the directions of the system coordinates and the operator $\mathbf{h}$ defines the relation between the output variables $\mathbf{y}$ and the coordinates. A typical example for the system outputs is the end-effector position of a manipulator. For an underactuated system, we have $n - m - s > 0$.

2.2 Inverse dynamics equation

Let $\mathbf{y}_d(t)$ be a smooth desired trajectory for the output variables, which is defined over a finite time interval $[t_0, t_f]$. This means that $\mathbf{y}_d(t)$ is constant for $t \notin [t_0, t_f]$. We also assume that the trajectory and its derivatives remain smooth up to order 2 at t_0 and t_f, i.e., $\dot{\mathbf{y}}_d(t_0) = \dot{\mathbf{y}}_d(t_f) = \mathbf{0}$ and $\ddot{\mathbf{y}}_d(t_0) = \ddot{\mathbf{y}}_d(t_f) = \mathbf{0}$. The control objective is to define the control inputs $\mathbf{u}(t)$ so that the condition

$$\mathbf{y}(t) = \mathbf{y}_d(t) \tag{2}$$

is satisfied $\forall t$. Inserting (2) in (1c) yields the so-called trajectory or servo-constraint $\mathbf{y}_d(t) - \mathbf{h}(\mathbf{q}) = \mathbf{0}$. The external forces in $\mathbf{g}$ may explicitly depend on time, but we consider that their values only vary on the interval $[t_0, t_f]$.

The feedforward control $\mathbf{u}_{ff}(t)$ should satisfy the following equation which states the inverse model

$$\begin{aligned} \mathbf{M}(\mathbf{q})\ddot{\mathbf{q}} + \mathbf{g}(\mathbf{q}, \dot{\mathbf{q}}, t) + \mathbf{H}(\mathbf{q})\,\boldsymbol{\mu} &= \mathbf{0} && \text{(3a)} \\ \mathbf{\Psi}(\mathbf{q}, t) &= \mathbf{0} && \text{(3b)} \end{aligned}$$

with

$$\boldsymbol{\mu} = \begin{bmatrix} \boldsymbol{\lambda} \\ \mathbf{u}_{ff} \end{bmatrix}, \quad \mathbf{\Psi} = \begin{bmatrix} \mathbf{\Phi}(\mathbf{q}) \\ \mathbf{y}_d(t) - \mathbf{h}(\mathbf{q}) \end{bmatrix}, \quad \mathbf{H} = [\mathbf{\Phi}_{\mathbf{q}}^T \; -\mathbf{A}] \tag{4}$$

Due to the presence of the trajectory constraint, we have $\mathbf{H} \neq \mathbf{\Psi}_{\mathbf{q}}^T$.

In the following developments, it is assumed that the index of the differential-algebraic equation (3) is 3, i.e., the matrix

$$\begin{bmatrix} \mathbf{M} & \mathbf{H} \\ \mathbf{\Psi}_{\mathbf{q}} & \mathbf{0} \end{bmatrix} \tag{5}$$

is non-singular. Blajer and Kolodziejczyk [19] and Seifried and Blajer [21] have shown that the index may actually be higher than 3 in the case of a so-called tangent realization of a trajectory constraint. This situation will not be covered here.

We also consider that, for every time t, the system has an equilibrium point $\mathbf{q}_e(t)$ which is a solution of the algebraic system

$$\begin{aligned} \mathbf{g}(\mathbf{q}_e, \mathbf{0}, t) + \mathbf{H}(\mathbf{q}_e)\,\boldsymbol{\mu} &= \mathbf{0} && \text{(6a)} \\ \mathbf{\Psi}(\mathbf{q}_e, t) &= \mathbf{0} && \text{(6b)} \end{aligned}$$

In order to guarantee the solvability of Eq. (6), we assume that the tangent matrix

$$\begin{bmatrix} \mathbf{K}_t & \mathbf{H} \\ \mathbf{\Psi}_{\mathbf{q}} & \mathbf{0} \end{bmatrix} \tag{7}$$

is non-singular, where $\mathbf{K}_t = \partial(\mathbf{g} + \mathbf{H}\boldsymbol{\mu})/\partial\mathbf{q}$ is the tangent stiffness matrix of the system.

2.3 Boundary conditions

An elimination of the algebraic constraint in Eq. (3) would lead to a second-order ordinary differential equation (ODE) of dimension $n-m-s$, which would represent the internal dynamics of the system, see, e.g., [13]. This internal dynamics might be stable or unstable. In flexible multibody dynamics, the internal dynamics is often unstable and, in this case, if Eq. (3) is solved by forward time integration from specified values of $\mathbf{q}(t_0)$ and $\dot{\mathbf{q}}(t_0)$ at the initial time t_0, the solution would be unbounded. Such an unbounded solution would require large control efforts and be useless for the practical implementation of a feedforward control law.

However, a bounded solution can be found if a non-causal solution is considered. This means that the control inputs should start before the beginning of the prescribed trajectory in a pre-actuation phase and continue after its end in a post-actuation phase. According to the stable inversion method, this non-causal solution can be evaluated as the solution of a two-point boundary value problem [14, 15]. The zero-dynamics is a useful concept for the definition of the boundary conditions.

Let us introduce the $2n$-dimensional vector of state variable $\mathbf{x}(t)$ defined as

$$\mathbf{x}(t) = \begin{bmatrix} \mathbf{q}(t) \\ \dot{\mathbf{q}}(t) \end{bmatrix} \tag{8}$$

The state variables have to satisfy $m+s$ constraints at the position level and $m+s$ constraints at the velocity level, which results in a total of $2(m+s)$ algebraic constraints

$$\mathbf{\Psi}^*(\mathbf{x},t) = \begin{bmatrix} \mathbf{\Psi}(\mathbf{q},t) \\ \mathbf{\Psi}_{\mathbf{q}}(\mathbf{q},t)\,\dot{\mathbf{q}} + \mathbf{\Psi}_t(\mathbf{q},t) \end{bmatrix} = \mathbf{0} \tag{9}$$

The internal dynamics manifold of dimension $2(n-m-s)$ is the set of points in the state space which satisfy this set of constraints.

The zero-dynamics is the internal dynamics under the constraint that the output is kept constant [5, 6]. In our case, this condition is observed for $t < t_0$ (resp. $t > t_f$), and the zero-dynamics is thus investigated about two particular equilibrium points

$$\mathbf{x}_e(t_i) = \begin{bmatrix} \mathbf{q}_e(t_i) \\ \mathbf{0} \end{bmatrix}, \quad t_i = t_0, t_f \tag{10}$$

A system is nonminimum phase if its zero-dynamics is unstable [5, 6]. The stable manifold W_i^s of dimension n^s is the set of points of the zero-dynamics manifold from which the zero-dynamics converges to the equilibrium $\mathbf{x}_e(t_i)$ for $t \to +\infty$, while the unstable manifold W_i^u of dimension n^u is the set of points from which the zero-dynamics converges to the equilibrium $\mathbf{x}_e(t_i)$ for $t \to -\infty$.

Let us assume that the equilibrium is hyperbolic, which means that the linearized zero-dynamics has no eigenvalue on the imaginary axis and that $n^s + n^u$ is equal to the dimension of the internal dynamics $2(n-m-s)$. As illustrated in Fig. 2, a stable inversion method should provide a trajectory which evolves on the unstable manifold for $t < t_0$ and on the stable manifold for $t > t_f$. Even though the trajectory is defined in the interval $[t_0, t_f]$, the zero-dynamics is usually active outside of that interval. In order to drive the zero-dynamics, the control inputs should also be activated during the pre- and post-actuation phases. In practice, one defines $T_0 \leq t_0$ as the beginning of the pre-actuation phase and $T_f \geq t_f$ as the end of the post-actuation phase. Therefore, the boundary conditions of the problem are written as

$$\mathbf{x}(T_0) \in W_0^u, \quad \mathbf{x}(T_f) \in W_f^s \tag{11}$$

On the zero-dynamics manifold, the first and second conditions represent n^s and n^u additional constraints, respectively, so that a total of $n^s + n^u = 2(n-m-s)$ additional constraints

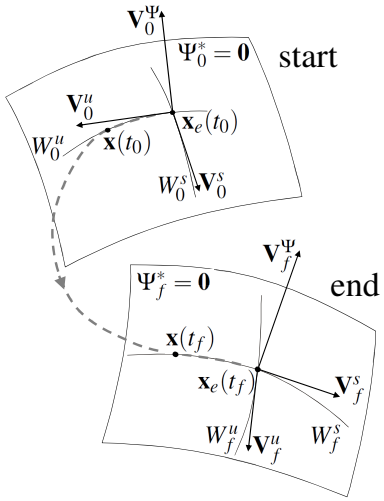

Figure 2: Boundary conditions for the zero-dynamics.

are defined by Eq. (11). In the special case of a stable zero-dynamics, W_f^s spans the whole state space, W_0^u is a zero-dimensional subspace, and Eq. (11) boils down to a initial condition $\mathbf{x}(T_0) = \mathbf{x}_e(t_0)$.

Since the geometry of the manifolds W_0^u and W_f^s can be rather complex in practical applications, a simplified definition of the boundary conditions can be based on the stable and unstable eigenspaces of the linearized zero-dynamics about the equilibrium point $\mathbf{x}_e(t_i)$

$$\mathbf{M}\,\Delta\ddot{\mathbf{q}} + \mathbf{C}_t\,\Delta\dot{\mathbf{q}} + \mathbf{K}_t\,\Delta\mathbf{q} + \mathbf{H}\,\Delta\boldsymbol{\mu} = \mathbf{0} \tag{12a}$$

$$\boldsymbol{\Psi}_\mathbf{q}\,\Delta\mathbf{q} = \mathbf{0} \tag{12b}$$

with $\Delta\mathbf{q}(t) = \mathbf{q}(t) - \mathbf{q}_e(t_i)$, $\mathbf{C}_t = \partial\mathbf{g}/\partial\dot{\mathbf{q}}$ and $\mathbf{K}_t = \partial(\mathbf{M}\ddot{\mathbf{q}} + \mathbf{g} + \mathbf{H}\,\boldsymbol{\mu})/\partial\mathbf{q}$. This system can be reformulated in state-space form as

$$\mathbf{E}\begin{bmatrix} \Delta\dot{\mathbf{x}} \\ \Delta\dot{\boldsymbol{\mu}} \end{bmatrix} = \mathbf{A}^*\begin{bmatrix} \Delta\mathbf{x} \\ \Delta\boldsymbol{\mu} \end{bmatrix} \tag{13}$$

with

$$\mathbf{E} = \begin{bmatrix} \mathbf{I} & \mathbf{0} & \mathbf{0} \\ \mathbf{0} & \mathbf{M} & \mathbf{0} \\ \mathbf{0} & \mathbf{0} & \mathbf{0} \end{bmatrix},\ \mathbf{A}^* = \begin{bmatrix} \mathbf{0} & \mathbf{I} & \mathbf{0} \\ -\mathbf{K}_t & -\mathbf{C}_t & -\mathbf{H} \\ \boldsymbol{\Psi}_\mathbf{q} & \mathbf{0} & \mathbf{0} \end{bmatrix} \tag{14}$$

Observing that the matrix $\mathbf{E}$ has a rank-deficiency, the generalized eigenvalue problem

$$(\mathbf{A}^* - \sigma\mathbf{E})\begin{bmatrix} \mathbf{v}^x \\ \mathbf{v}^\mu \end{bmatrix} = \mathbf{0} \tag{15}$$

has $2(n - m - s) = n^s + n^u$ finite eigenvalues. Since the equilibrium point is hyperbolic, none of the eigenvalues are on the imaginary axis. In the $2n$-dimensional state space, at the equilibrium $\mathbf{x}_e(t_i)$, with $t_i = t_0, t_f$, the n^s-dimensional stable eigenspace $\mathbf{V}_i^s$ collects the eigenvectors with eigenvalues in the left-half plane, the n^u-dimensional unstable eigenspace $\mathbf{V}_i^u$ collects the eigenvectors with eigenvalues in the right-half plane, and the $2(m + s)$-dimensional constraint gradient subspace $\mathbf{V}_i^\Psi = \boldsymbol{\Psi}_\mathbf{x}^{*,T}$. By construction, the $2n \times 2n$ matrix $[\mathbf{V}_i^s \quad \mathbf{V}_i^u \quad \mathbf{V}_i^\Psi]$ is regular

and its columns span the whole state space. Therefore, any increment $\Delta\mathbf{x}$ can be decomposed in this non-orthogonal basis as

$$\Delta\mathbf{x}(t) = \mathbf{V}_i^s\,\boldsymbol{\xi}_i^s(t) + \mathbf{V}_i^u\,\boldsymbol{\xi}_i^u(t) + \mathbf{V}_i^\Psi\,\boldsymbol{\xi}_i^\Psi(t) \tag{16}$$

Based on this change of variable, the linearized form of the $n^s + n^u$ boundary conditions in Eq. (11) is

$$\boldsymbol{\xi}_0^s(T_0) = \mathbf{0}, \quad \boldsymbol{\xi}_f^u(T_f) = \mathbf{0} \tag{17}$$

In addition, the conditions $\boldsymbol{\xi}_0^\Psi(T_0) = \mathbf{0}$ and $\boldsymbol{\xi}_f^\Psi(T_f) = \mathbf{0}$ also needs to be satisfied by the solution. In practice, Eq. (17) can be replaced by the following equivalent and final form of the linearized boundary conditions for Eq. (3)

$$\mathbf{P}_0^{u,T}\,(\mathbf{x}(T_0) - \mathbf{x}_e(t_0)) = \mathbf{0}, \quad \mathbf{P}_f^{s,T}\,(\mathbf{x}(T_f) - \mathbf{x}_e(t_f)) = \mathbf{0} \tag{18}$$

where $\mathbf{P}_0^u$ and $\mathbf{P}_f^s$ are null space matrices defined as $\mathbf{P}_0^u = \text{null}([\mathbf{V}_0^u \quad \mathbf{V}_0^\Psi]^T)$ and $\mathbf{P}_f^s = \text{null}([\mathbf{V}_f^s \quad \mathbf{V}_f^\Psi]^T)$.

3 Multiple shooting method

This section presents a multiple shooting method to solve the two-point boundary value formed by the DAE (3) with the linearized boundary conditions (18). Hence, this DAE stable inversion method does not require any reformulation of the problem in input-output normal form.

The time interval $[T_0, T_f]$ is discretized into N subintervals $[t^{(k)}, t^{(k+1)}]$, $k = 1, \ldots, N$. The DAE is then solved independently on each interval by forward time integration using an approximate initial value $\mathbf{q}_0^{(k)}$, $\dot{\mathbf{q}}_0^{(k)}$. This integration can be performed even if the internal dynamics is unstable, provided that the shooting interval is small enough to avoid a blow-up of the solution. The numerical integration algorithm provides a solution $\mathbf{q}^{(k)}(t; \mathbf{q}_0^{(k)}, \dot{\mathbf{q}}_0^{(k)})$, $\dot{\mathbf{q}}^{(k)}(t; \mathbf{q}_0^{(k)}, \dot{\mathbf{q}}_0^{(k)})$, $\boldsymbol{\mu}^{(k)}(t; \mathbf{q}_0^{(k)}, \dot{\mathbf{q}}_0^{(k)})$ over the interval $[t^{(k)}, t^{(k+1)}]$. Continuity conditions are imposed on the defect between two successive subintervals

$$\mathbf{q}^{(k)}(t^{(k+1)}; \mathbf{q}_0^{(k)}, \dot{\mathbf{q}}_0^{(k)}) = \mathbf{q}_0^{(k+1)} \tag{19a}$$

$$\dot{\mathbf{q}}^{(k)}(t^{(k+1)}; \mathbf{q}_0^{(k)}, \dot{\mathbf{q}}_0^{(k)}) = \dot{\mathbf{q}}_0^{(k+1)} \tag{19b}$$

for $k = 1, \ldots, N$. The situation is illustrated in Fig. 3 with the compact notation $\mathbf{q}_f^{(k)} = \mathbf{q}^{(k)}(t^{(k+1)}; \mathbf{q}_0^{(k)}, \dot{\mathbf{q}}_0^{(k)})$. The unknowns of the problem are the $2n(N+1)$ variables collected in the vector

$$\mathbf{z} = (\mathbf{q}_0^{(1)}; \dot{\mathbf{q}}_0^{(1)}; \ldots; \mathbf{q}_0^{(N+1)}; \dot{\mathbf{q}}_0^{(N+1)}) \tag{20}$$

These unknowns have to verify the $2nN$ continuity conditions in Eq. (19) and the $n^s + n^u = 2(n-m-s)$ linearized boundary conditions in Eq. (18). Additionally, the $2(m+s)$ constraints at position and velocity levels for the initial state

$$\begin{bmatrix} \boldsymbol{\Psi}_\mathbf{q}(\mathbf{q}_e(t_0)) & \mathbf{0} \\ \mathbf{0} & \boldsymbol{\Psi}_\mathbf{q}(\mathbf{q}_e(t_0)) \end{bmatrix} \begin{bmatrix} \mathbf{q}_0^{(1)} - \mathbf{q}_e(t_0) \\ \dot{\mathbf{q}}_0^{(1)} \end{bmatrix} = \mathbf{0} \tag{21}$$

are needed to obtain a well-posed numerical problem. Thus, a system of $2n(N+1)$ nonlinear algebraic equations $\mathbf{f}(\mathbf{z}) = \mathbf{0}$ is obtained by combining Eqs. (18,19,21). This problem can be solved using a Newton iterative method.

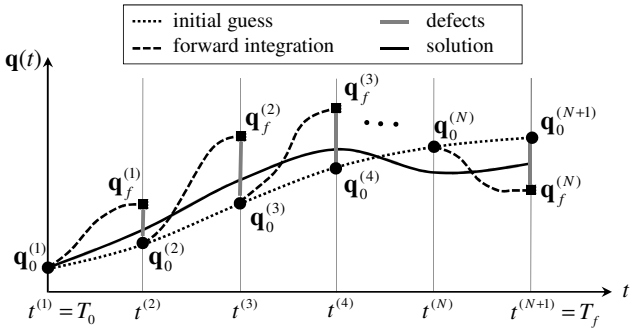

Figure 3: Multiple shooting method.

In order to initiate the Newton iterations, the initial guess $\mathbf{z}_0$ is defined in the following way. For $k = 1, \ldots, N+1$, the vectors $\mathbf{q}_0^{(k)}$ and $\dot{\mathbf{q}}_0^{(k)}$ are initialized as

$$\mathbf{q}_0^{(k)} = \mathbf{q}_e(t^{(k)}) \tag{22}$$

$$\dot{\mathbf{q}}_0^{(k)} = \frac{d\mathbf{q}_e}{dt}(t^{(k)}) \tag{23}$$

The equilibrium configuration $\mathbf{q}_e(t^{(k)})$ is found by solving the equilibrium condition at time $t^{(k)}$ defined by Eq. (6). This is again a nonlinear problem which is solved using a Newton iterative procedure and the value at the previous interval $\mathbf{q}_0^{(k-1)}$ is used as the initial guess. The time derivative of $\mathbf{q}_e$ is found by solving the time differentiated form of the equilibrium condition (6) as

$$\mathbf{K}_t \frac{d\mathbf{q}_e}{dt} + \mathbf{g}_t + \mathbf{H}\,\frac{d\boldsymbol{\mu}}{dt} = \mathbf{0} \tag{24}$$

$$\boldsymbol{\Psi}_{\mathbf{q}}\dot{\mathbf{q}}_e + \boldsymbol{\Psi}_t = \mathbf{0} \tag{25}$$

In this way, the initial guess is such that the initial conditions satisfy the algebraic constraints of the DAE (3) at the position and velocity levels.

The Newton scheme requires the gradient of the function $\mathbf{f}(\mathbf{z})$, which is composed of the boundary conditions and the continuity conditions. The derivative of the linearized boundary conditions with respect to $\mathbf{q}_0^{(1)}$, $\dot{\mathbf{q}}_0^{(1)}$, $\mathbf{q}_0^{(N+1)}$ and $\dot{\mathbf{q}}_0^{(N+1)}$ is easily obtained from the matrices $\mathbf{D}_t$, $\mathbf{P}^u$ and $\mathbf{P}^s$. The derivative of the continuity conditions requires the evaluation of the sensitivities of the final state with respect to the initial state $\partial\mathbf{q}_f^{(k)}/\partial\mathbf{q}_0^{(k)}$, $\partial\mathbf{q}_f^{(k)}/\partial\dot{\mathbf{q}}_0^{(k)}$, $\partial\dot{\mathbf{q}}_f^{(k)}/\partial\mathbf{q}_0^{(k)}$ and $\partial\dot{\mathbf{q}}_f^{(k)}/\partial\dot{\mathbf{q}}_0^{(k)}$ for each shooting subinterval.

4 Time integration method

At each iteration of the Newton procedure, the evaluation of the function $\mathbf{f}(\mathbf{z})$ requires N forward time integrations of the DAE (3) with approximate initial conditions $\mathbf{q}_0^{(k)}$, $\dot{\mathbf{q}}_0^{(k)}$ over relatively short shooting subintervals.

The multiple shooting algorithm does not guarantee that, during the Newton iterations, the initial conditions satisfy the constraints at position and velocity levels. Usually, time integration schemes for DAEs do not behave well if the initial values do not satisfy the constraints. For this reason, a classical projection algorithm, see, e.g., [33], can be implemented in order to

obtain corrected values $\mathbf{q}_0^{(k)*}$, $\dot{\mathbf{q}}_0^{(k)*}$ which satisfy the constraints. In our case, the constraints at position and velocity levels are satisfied for the initial guess and for the final solution. Usually, the initial values also stay in a close neighbourhood of the constraint during the Newton iterations. Therefore, this projection step can often be skipped in practice.

In order to reduce the influence of perturbations and to eliminate transient numerical oscillations, the DAE is formulated in index-2 form according to the Gear-Gupta-Leimkuhler method [30]. The generalized-α solver [26, 28] is used to solve the resulting index-2 problem as in [29]. The index-2 form of Eq. (3) involves the constraints both at position and velocity levels

$$\begin{aligned} \mathbf{M}(\mathbf{q})(\dot{\mathbf{q}} - \mathbf{v}) + \mathbf{H}(\mathbf{q})\boldsymbol{\eta} &= \mathbf{0} && (26)\\ \mathbf{M}(\mathbf{q})\dot{\mathbf{v}} + \mathbf{g}(\mathbf{q}, \mathbf{v}, t) + \mathbf{H}(\mathbf{q})\boldsymbol{\mu} &= \mathbf{0} && (27)\\ \boldsymbol{\Psi}(\mathbf{q}, t) &= \mathbf{0} && (28)\\ \boldsymbol{\Psi}_{\mathbf{q}}(\mathbf{q}, t)\,\mathbf{v} + \boldsymbol{\Psi}_t(\mathbf{q}, t) &= \mathbf{0} && (29) \end{aligned}$$

and the additional vector of multipliers $\boldsymbol{\eta}$ can compensate for the increased number of equations in the problem. It can be shown that $\boldsymbol{\eta}$ vanishes identically for the analytical solution so that this system yields the same solution as the original problem with $\mathbf{v} = \dot{\mathbf{q}}$.

Considering that the time step size h is constant, the numerical scheme is defined by the following set of equations at time step $i+1$

$$\begin{aligned} \mathbf{M}(\mathbf{q}_{i+1})(\dot{\mathbf{q}}_i - \mathbf{v}_i) + \mathbf{H}(\mathbf{q}_{i+1})\boldsymbol{\eta}_{i+1} &= \mathbf{0}\\ \mathbf{M}(\mathbf{q}_{i+1})\dot{\mathbf{v}}_{i+1} + \mathbf{g}(\mathbf{q}_{i+1}, \mathbf{v}_{i+1}, t_{i+1}) + \mathbf{H}(\mathbf{q}_{i+1})\boldsymbol{\mu}_{i+1} &= \mathbf{0}\\ \boldsymbol{\Psi}(\mathbf{q}_{i+1}, t_{i+1}) &= \mathbf{0}\\ \boldsymbol{\Psi}_{\mathbf{q}}(\mathbf{q}_{i+1}, t_{i+1})\,\mathbf{v}_{i+1} + \boldsymbol{\Psi}_t(\mathbf{q}_{i+1}, t_{i+1}) &= \mathbf{0} \end{aligned}$$

Those discrete equations are combined with the generalized-α integration formulae

$$\begin{aligned} \mathbf{q}_{i+1} &= \mathbf{q}_i + h\dot{\mathbf{q}}_i + h^2(0.5 - \beta)\mathbf{a}_i + h^2\beta\mathbf{a}_{i+1}\\ \mathbf{v}_{i+1} &= \mathbf{v}_i + h(1-\gamma)\mathbf{a}_i + h\gamma\mathbf{a}_{i+1}\\ (1-\alpha_m)\mathbf{a}_{i+1} + \alpha_m\mathbf{a}_i &= (1-\alpha_f)\dot{\mathbf{v}}_{i+1} + \alpha_f\dot{\mathbf{v}}_i \end{aligned}$$

where γ, β, α_m and α_f are numerical parameters of the generalized-α method, and $\mathbf{a}_i$ is a pseudo-acceleration variable, which approximates $\dot{\mathbf{v}}(t_i + (\alpha_m - \alpha_f)h)$, see [34]. The numerical parameters can be chosen to combine unconditional stability and second-order accuracy. According to [26], they can be defined from a single design parameter $\rho_\infty \in [0, 1)$, which represents the spectral radius at infinite frequencies. The algorithm requires at each time step the solution of a system of $2n + 2m$ nonlinear equations for the independent variables $\mathbf{v}_{i+1}$, $\dot{\mathbf{q}}_i$, $\boldsymbol{\mu}_{i+1}$ and $\boldsymbol{\eta}_{i+1}$, since the other variables $\mathbf{q}_{i+1}$, $\dot{\mathbf{v}}_{i+1}$, and $\mathbf{a}_{i+1}$ can easily be expressed in terms of these variables using the linear time integration formulae.

The initial value $\dot{\mathbf{v}}_0$ is obtained by solving the equation of motion with the constraints at acceleration level

$$\begin{aligned} \mathbf{M}\dot{\mathbf{v}}_0 + \mathbf{g}(\mathbf{q}_0, \mathbf{v}_0, t_0) + \mathbf{H}(\mathbf{q}_0)\boldsymbol{\mu}_0 &= \mathbf{0}\\ \boldsymbol{\Psi}_{\mathbf{q}}(\mathbf{q}_0, t_0)\,\dot{\mathbf{v}}_0 + \frac{d\boldsymbol{\Psi}_{\mathbf{q}}}{dt}(\mathbf{q}_0, \mathbf{v}_0, t_0)\,\mathbf{v}_0 + \frac{d\boldsymbol{\Psi}_t}{dt}(\mathbf{q}_0, \mathbf{v}_0, t_0) &= \mathbf{0} \end{aligned}$$

The initial value $\mathbf{a}_0$ can be defined as $\mathbf{a}_0 = \dot{\mathbf{v}}_0$, which is a crude approximation, or as $\mathbf{a}_0 = \dot{\mathbf{v}}(t_0 + (\alpha_m - \alpha_f)h)$, which is a more accurate estimate. In the following, this second and more accurate option is considered so that the influence of perturbations in the initial phase of each time integration subinterval is reduced. For that purpose, the variable $\dot{\mathbf{v}}(t_0 + (\alpha_m - \alpha_f)h)$ is obtained by performing one time step of size $(\alpha_m - \alpha_f)h$ using the undamped Newmark

algorithm, which is a special case of the generalized-α algorithm with the numerical parameters defined as $\beta = 0.25$, $\gamma = 0.5$, $\alpha_m = \alpha_f = 0$.

The computation of the sensitivity of the final state with respect to the initial state is based on a direct differentiation of the time integration code, see, e.g., [31]. This task is usually affordable because the only source of nonlinearity in the code comes from the equation of motion, whose linearized form is often readily available in implicit codes. Compared to a finite difference scheme, this approach can save a significant amount of computational time.

5 Numerical examples

The proposed DAE stable inversion method is applied for two planar and flexible manipulators which are nonminimum phase, i.e., their inverse dynamics is unstable. In either case, the equation of motion in DAE form is obtained according to a nonlinear finite element approach based on absolute coordinates [35].

5.1 Serial manipulator with one passive joint

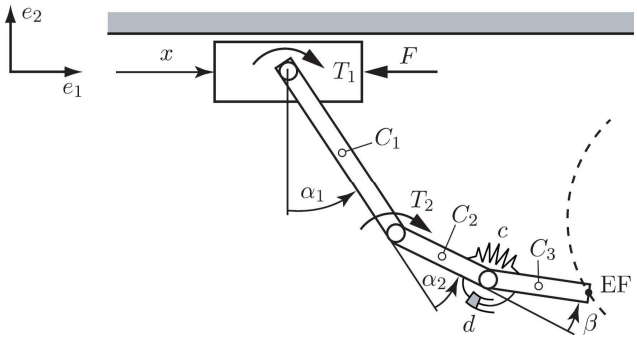

Figure 4: Planar serial manipulator with one passive joint

An underactuated manipulator with one passive joint and kinematic redundancy is considered as shown in Fig. 4. This problem has already been studied in [36]. The manipulator has four degrees of freedom in the horizontal plane and consists of a cart on which a chain of three rigid arms is mounted. It is actuated by $s = 3$ control inputs $\mathbf{u} = (F, T_1, T_2)^T$, where F is the force exerted on the cart, T_1 and T_2 are the joint torques. The arms have lengths l_1 and $l_2 = l_3$, masses m_1 and $m_2 = m_3$ and inertias I_1, $I_2 = I_3$. The third arm is connected by a passive joint to arm 2, which is supported by a parallel spring-damper combination with spring constant c and damping coefficient d. The physical parameters of the manipulator are summarized in Table 1.

Following the nonlinear finite element formalism [35], the manipulator is described using the absolute coordinates of some nodes of the system, as shown in Fig. 5, with

$$\mathbf{q} = (x_0, x_1, y_1, \theta_1, x_2, y_2, x_3, y_3, \theta_3, x_4, y_4, x_5, y_5, \theta_5, x_6, y_6)^T,$$

where x_i and y_i are the translations of node i along axes e_1 and e_2, respectively, and θ_i is the absolute orientation angle of a coordinate system attached to node i. Those $n = 16$ coordinates

cart	$m_c = 3\,\mathrm{kg}$		
arm 1	$m_1 = 6.875\,\mathrm{kg}$	$I_1 = 0.5743\,\mathrm{kgm}^2$	$l_1 = 1.0\,\mathrm{m}$
arm 2	$m_2 = 3.438\,\mathrm{kg}$	$I_2 = 0.0723\,\mathrm{kgm}^2$	$l_2 = 0.5\,\mathrm{m}$
arm 3	$m_3 = 3.438\,\mathrm{kg}$	$I_3 = 0.0723\,\mathrm{kgm}^2$	$l_3 = 0.5\,\mathrm{m}$
passive joint	$c = 50\,\mathrm{Nm/rad}$	$d = 0.25\,\mathrm{Nms/rad}$	

Table 1: Parameters of the serial manipulator.

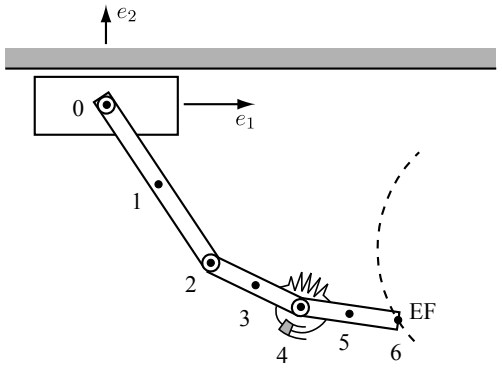

Figure 5: Underactuated serial manipulator: Discretization in absolute coordinates

are not independent but they have to satisfy $m = 12$ kinematic constraints. The relative angles α_1, α_2 and β defined in Fig. 4 satisfy $\alpha_1 = \theta_1$, $\alpha_2 = \theta_3 - \theta_1$, and $\beta = \theta_5 - \theta_3$.

The control goal is to force the cart and the end-effector to follow a predefined trajectory as closely as possible. The problem has three trajectory constraints that are imposed on the cart motion x_0, and on the end-effector positions (x_6, y_6), so that $\mathbf{y} = (x_0, x_6, y_6)^T$ describes the output of the manipulator and $\mathbf{h}(\mathbf{q})$ is a linear and boolean operator

$$\mathbf{h}(\mathbf{q}) = \begin{bmatrix} 1 & 0 & \dots & 0 & 0 & 0 \\ 0 & 0 & \dots & 0 & 1 & 0 \\ 0 & 0 & \dots & 0 & 0 & 1 \end{bmatrix} \mathbf{q} \tag{30}$$

The trajectories are shown in Fig. 6. The system has $s = 3$ trajectory constraints. The end-effector point EF should follow a half-circular trajectory. The center of the half-circle is at position $(0.0, -1.5)$[m] and the radius is 1.0 m. Also, the cart should move from the starting position -1.0 m to the final position 1.0 m. The end-effector point and the cart should follow the trajectory in the short time period of 1.5 s, which describes an aggressive manoeuver. The pre-actuation period is 0.2 s and the post-actuation period is 0.3 s long.

In this example, the internal dynamics, which is the remaining dynamics when all output variables are imposed, can be parameterized by the angle of the passive joint β. Therefore, the state space of the internal dynamics is two-dimensional and can be investigated in the β, $\dot{\beta}$ plane. In the initial and final configurations, the solution of Eq. (15) reveals that the internal dynamics has one stable eigenvalue and one unstable eigenvalue. The unstable eigenvalue is real and located at 28.30 rad/s. The internal dynamics of the system can be explicitly obtained as a second-order ODE for the coordinate β if the equation of motion is formulated in input-output normal form, see, e.g., [18]. An advantage of the proposed DAE stable inversion approach is that the equations are treated in standard DAE form without the need to derive such an

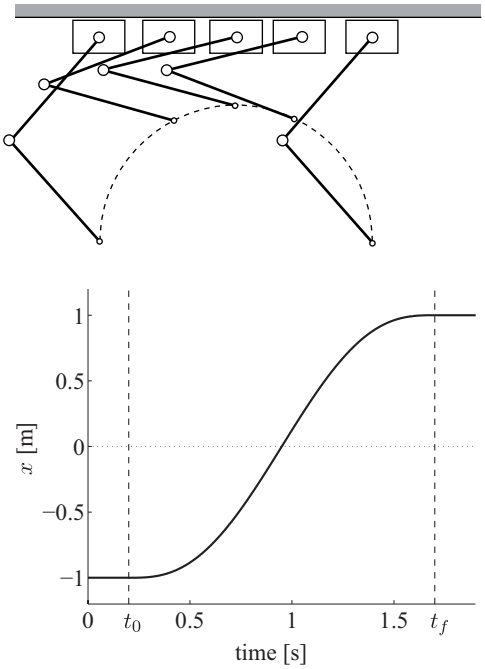

Figure 6: Serial manipulator: Desired trajectory

input-output normal form.

The DAE stable inversion method is used with $N = 40$ shooting subintervals, 10 time steps in each subinterval and the parameters of the generalized-α method specified according to [26] with the spectral radius at infinity $\rho_\infty = 0.8$. The size of the time steps and of the shooting subintervals are constant. In this example, it is observed that a numerical solution could only be obtained for $N \geq 32$, otherwise the shooting subintervals would be too long and the forward integration could not be achieved successfully due to the instability of the internal dynamics. For $N = 40$, the solution is found after 6 Newton iterations.

The results are shown in Fig. 7. In the β, $\dot{\beta}$ plane, the internal dynamics evolves on the unstable manifold for $t \leq t_0$ (pre-actuation phase) and on the stable manifold for $t \geq t_f$ (post-actuation phase). These results are in agreement with the results obtained in [36] using a DAE optimal control formulation and a direct transcription algorithm. Also, they agree with [18] where the internal dynamics is derived explicitly as an ODE and the boundary value problem is solved using a finite difference scheme. A comparison between the stable inversion method presented here with a time grid including 401 points and the direct transcription optimal control method [36] with a time grid of only 100 points shows that the stable inversion method runs about 50 times faster using the same computer and a similar software environment. This demonstrate the ability of the proposed DAE stable inversion method to solve efficiently inverse dynamics problems for nonminimum phase systems.

Let us study the influence of the spring and damper coefficients of the passive joint. In the limit case $c = 0$ Nm/rad and $d = 0$ Nms/rad, the equilibrium points of the internal dynamics is not hyperbolic anymore and the proposed method is not applicable. The presence of the spring is necessary to maintain a kind of controllability of the system. For the specified trajectory, we were not able to compute a solution for $c \leq 4$ Nm/rad and $d = 0$ Nms/rad. For $c = 5$ Nm/rad and $d = 0$ Nms/rad, a solution could be obtained and the resulting phase diagram is

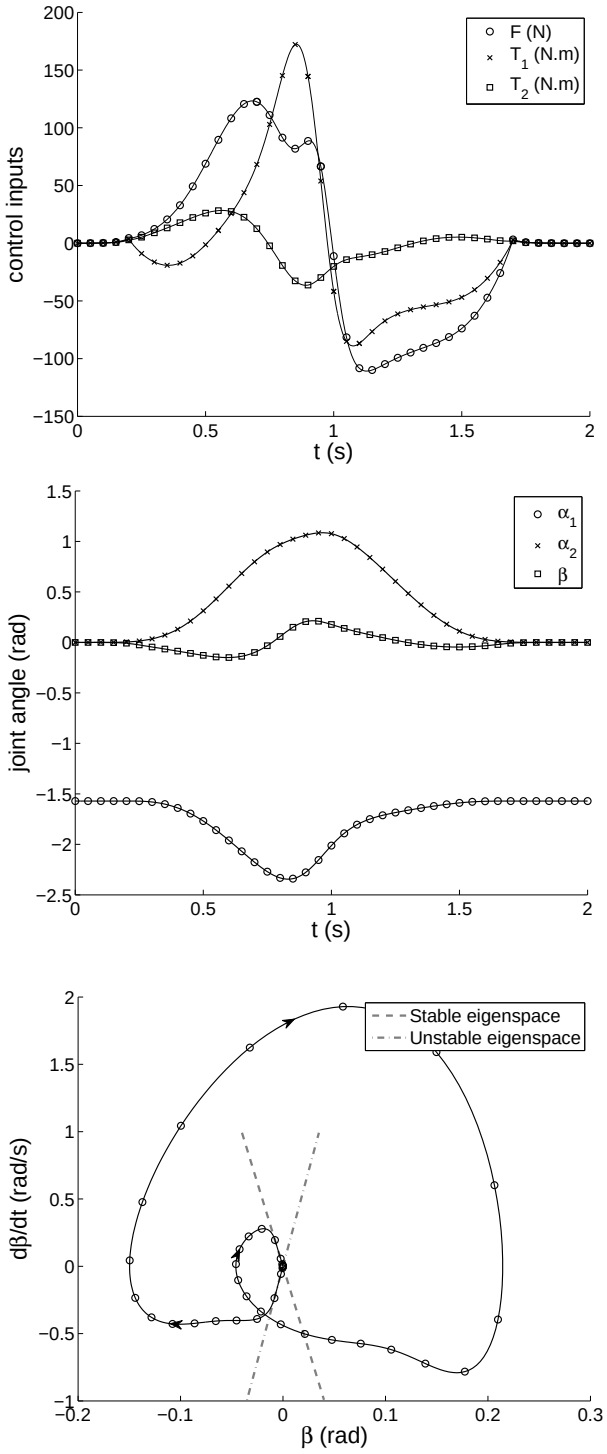

Figure 7: Serial manipulator, results for $c = 50$ Nm/rad and $d = 0.25$ Nms/rad.

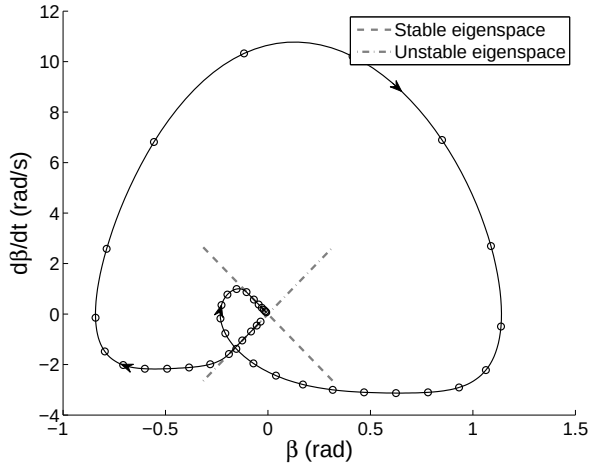

Figure 8: Serial manipulator, results for $c = 5$ Nm/rad and $d = 0$ Nms/rad.

given in Fig. 8. One observes that the amplitude of the internal dynamics β gets larger when the spring-damper combination is weakened.

5.2 Flexible parallel manipulator

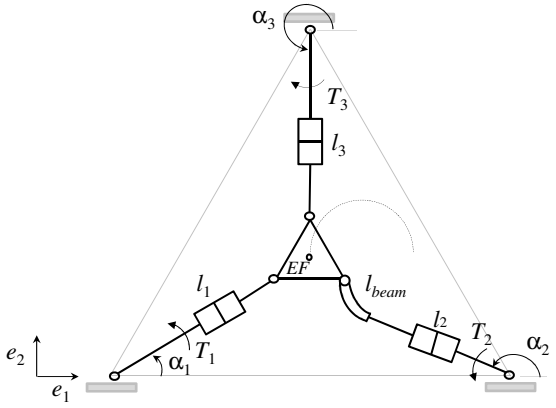

Figure 9: Flexible parallel manipulator

A 3-RPR parallel manipulator [37] with one flexible body is considered, see Fig. 9. This machine is composed of three prismatic joints with variable lengths l_1, l_2 and l_3, a triangular rigid plate and a flexible beam with undeformed length l_{beam}. The beam is clamped to the prismatic joint at one extremity and it is hinged to the triangular plate at the other extremity. The manipulator moves in the horizontal plane and the plate center is the end-effector of the system. It is actuated by three control inputs, which are the three torques of the motorized hinges $\mathbf{u} = (T_1, T_2, T_3)^T$. If all structural members were rigid, the system would have 3 degrees of freedom and it would be fully actuated. However, due to the flexibility of the beam, it is a continuous and underactuated mechanical system. The outputs of the system are the effector

position and orientation $\mathbf{y} = (x_{\text{eff}}, y_{\text{eff}}, \theta_{\text{eff}})^T$. The plate should follow a half-circular trajectory with a radius of 0.1 m and the plate orientation should preserve its initial value $\theta_{\text{eff}} = 0$ for all time. The trajectory should be followed in a 2.2 s time period and the pre- and post-actuation phases are 0.15 s long.

The initial lengths of the prismatic joints are $l_1 = l_3$ and l_2. The flexible beam has undeformed length l_{beam}, $b \times d$ rectangular cross section, with b the out-of-plane thickness, Young modulus E, Poisson ratio ν, density ρ and structural damping coefficient ϵ. The plate has an equilateral triangular geometry with side length a, mass m and rotational inertia I. The physical parameters of this parallel manipulator are $l_1 = l_3 = 1.35$ m, $l_2 = 0.75$ m, $a = 0.5$ m, $m = 0.1$ kg, $I = 0.01$ kgm^2, $l_{beam} = 0.6$ m, $b = 0.04$ m, $d = 0.0015$ m, $E = 2.e11$ Pa, $\nu = 0.3$, $\rho = 2.e4$ kg/m^3, $\epsilon = 1.e\text{-}3$ s.

The equation of motion is derived using the nonlinear finite element method based on absolute coordinates [35] and the proposed algorithm deals with the dynamic equilibrium in standard DAE form. The geometrically exact planar beam model relies on a Cosserat formulation, i.e., it accounts for traction, shear and bending deformations. The formulation of the internal dynamics in ODE form would be rather intricate for this system, but is not required here. The problem is described using n coordinates, $m = 9$ kinematic constraints and $s = 3$ trajectory constraints.

If the flexible beam is discretized in space using one finite element, the number of coordinates is $n = 15$ and the internal dynamics of the discrete inverse model in state space is 6-dimensional. In the initial configuration, it has five stable eigenvalues and one unstable eigenvalue. The unstable eigenvalue is real and located at 25.31 rad/s. If the flexible beam is discretized in space using two finite elements, the number of coordinates is $n = 18$ and the internal dynamics of the discrete inverse model is 12-dimensional in state space. In the initial configuration, it has ten stable eigenvalues and two unstable eigenvalues. The unstable eigenvalues are real and located at 22.00 rad/s and 406.12 rad/s.

For the discrete system with a single finite element, the DAE stable inversion method is used with $N = 80$ shooting subintervals, 25 time steps in each subinterval and the parameters of the generalized-α method specified according to [26] with the spectral radius at infinity $\rho_\infty = 0.8$. For the discrete system with two finite elements, the presence of a high frequency unstable eigenvalue implies a strong restriction in the length of the shooting subintervals in order to avoid a blow-up of the numerical solution. In this case, the method is used with $N = 500$ shooting subintervals and 20 time steps in each subinterval, the other numerical parameters being unchanged. In either case, the results are found after less than 7 Newton iterations.

The results are shown in Fig. 10. Defining β as the relative angle between the two extremities of the beam, which thus represents the amplitude of the first bending mode, the internal dynamics is partially investigated in the β, $\dot{\beta}$ plane. However, this is only a truncated view of the full state space dynamics, which is either 6- or 12-dimensional depending on the selected finite element grid. If the results are affected by the number of elements, the control torques to be applied on the system appear weakly sensitive with respect to this parameter. In other words, in this example, the results obtained with one single element are already a reasonable approximation of the solution. Finally, the influence of the structural dissipation parameter has been checked. When $\epsilon = 0$ s, some eigenvalues of the internal dynamics are located on the imaginary axis and the system is not hyperbolic anymore. However, the eigenvalues on the imaginary axis are all simple. If they are treated as stable eigenvalues, the computation could be successfully achieved with the other physical and numerical parameters unchanged.

This second example demonstrates the ability of the proposed DAE stable inversion method to compute the inverse dynamics of nonminimum phase multibody systems with flexible arms and closed kinematic chains.

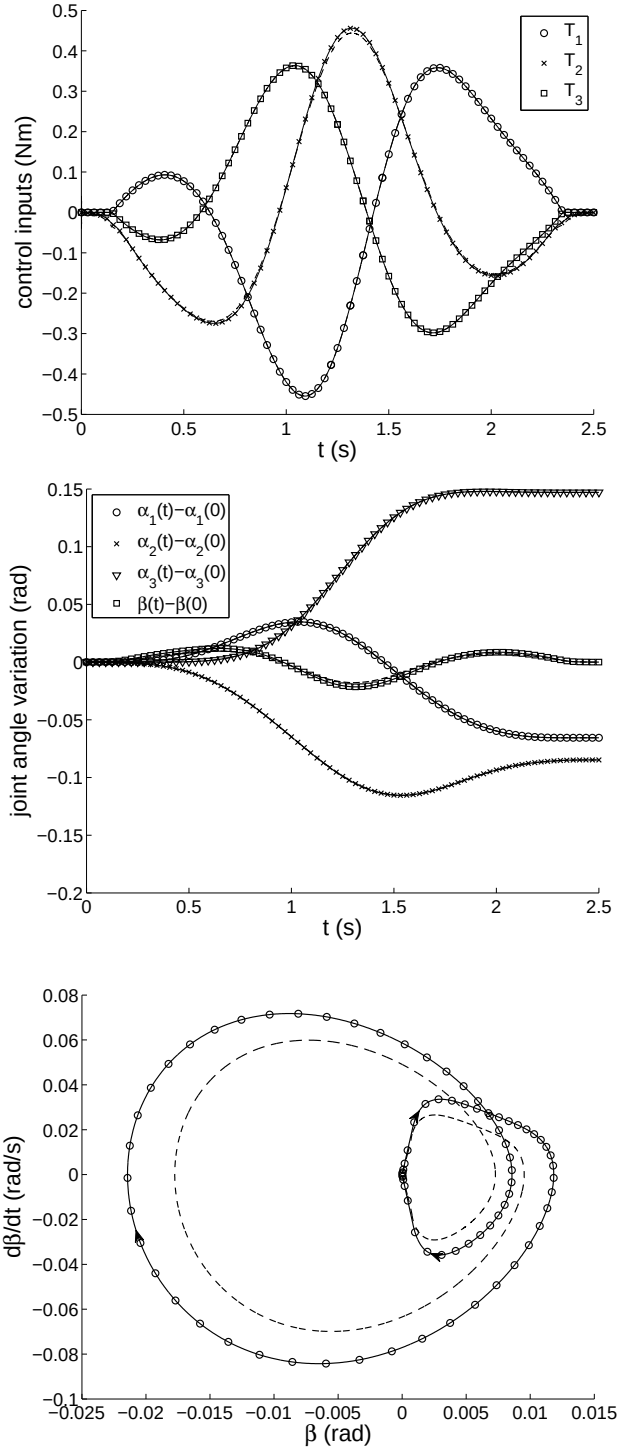

Figure 10: Results for the parallel manipulator (solid line: 1 finite element, dashed line: 2 finite elements).

6 Conclusions

Feedforward control schemes can take advantage of inverse dynamics techniques. Inverse models of flexible multibody systems are often nonminimum phase which means that their internal dynamics is unstable. Therefore, the inverse dynamics problem cannot be solved algebraically or by forward time integration. The stable inversion technique allows to obtain a stable but non-causal trajectory by solving a two-point boundary value problem. The boundary conditions impose that the trajectory starts from the unstable manifold in a pre-actuation phase and ends on the stable manifold in a post-actuation phase.

This paper proposes a DAE stable inversion approach which relies on the standard equation of motion of a flexible multibody system in DAE form. There is no need to derive the internal dynamics in ODE form. The DAE two-point boundary value problem is solved using a robust and efficient multiple shooting method. In each shooting subinterval, the algorithms relies on a forward time integration of the DAE in index-2 form using the generalized-α method and a sensitivity analysis of the final state with respect to the initial conditions based on a direct differentiation algorithm. The length of the subintervals is defined in order to avoid a blow-up of the solution which may result from the instability of the internal dynamics. The method has been successfully applied for the inverse dynamics analysis of flexible manipulators with serial and parallel kinematic topology. When the finite element grid is refined, high frequency and unstable eigenvalues may appear in the internal dynamics equation, which implies a strong restriction in the length of the shooting subintervals in order to avoid a blow-up of the solution. Therefore, the method is best suited to deal with low-frequency models.

References

[1] Cannon, H., and Schmitz, E., 1984. "Initial experiments on the end-point control of a flexible one-link robot". *International Journal of Robotics Research,* **3**(3), pp. 62–75.

[2] Book, W., 1993. "Controlled motion in an elastic world". *ASME Journal of Dynamic Systems, Measurement, and Control,* **115**(2B), pp. 252–261.

[3] Da Silva, M., Brüls, O., Swevers, J., Desmet, W., and Van Brussel, H., 2009. "Computer-aided integrated design for machines with varying dynamics". *Mechanism and Machine Theory,* **44**, pp. 1733–1745.

[4] Fliess, M., Lévine, J., Martin, P., and Rouchon, P., 1995. "Flatness and defect of nonlinear systems: Introductory theory and examples". *International Journal of Control,* **61**, pp. 1327–1361.

[5] Isidori, A., 1995. *Nonlinear Control Systems*, 3rd ed. Springer, London, UK.

[6] Sastry, S., 1999. *Nonlinear Systems: Analysis, Stability and Control*. Springer, New York.

[7] Van Nieuwstadt, M., and Murray, R., 1998. "Real-time trajectory generation for differentially flat systems". *International Journal of Robust Nonlinear Control,* **18**(11), pp. 995–1020.

[8] Asada, H., and Slotine, J.-J., 1986. *Robot Analysis and Control*. Wiley-Interscience.

[9] Spong, M., 1987. "Modeling and control of elastic joint robots". *ASME Journal of Dynamic Systems, Measurement, and Control,* **109**, pp. 310–319.

[10] Kwon, D., and Book, W., 1994. "A time-domain inverse dynamic tracking control of a single-link flexible manipulator". *ASME Journal of Dynamic Systems, Measurement, and Control,* **116**(2), pp. 193–200.

[11] Devasia, S., and Bayo, E., 1994. "Inverse dynamics of articulated flexible structures : Simultaneous trajectory tracking and vibration reduction". *Journal of Dynamics and Control,* **4**(3), pp. 299–309.

[12] Seifried, R., Held, A., and Dietmann, F., 2011. "Analysis of feed-forward control design approaches for flexible multibody systems". *Journal of System Design and Dynamics,* **5**(3), pp. 429–440.

[13] Seifried, R., Burkhardt, M., and Held, A., 2013. "Trajectory control of serial and parallel flexible manipulators using model inversion". In Multibody Dynamics: Computational Methods and Applications, Computational Methods in Applied Sciences, Volume 28, J. Samin and P. Fisette, eds., Springer.

[14] Devasia, S., Chen, D., and Paden, B., 1996. "Nonlinear inversion-based output tracking". *IEEE Transactions on Automatic Control,* **41**(7), pp. 930–942.

[15] Taylor, D., and Li, S., 2002. "Stable inversion of continuous-time nonlinear systems by finite-difference methods". *IEEE Transactions on Automatic Control,* **47**(3), pp. 537–542.

[16] Seifried, R., 2012. "Two approaches for feedforward control and optimal design of underactuated multibody systems". *Multibody System Dynamics,* **27**(1), pp. 75–93.

[17] Seifried, R., 2012. "Integrated mechanical and control design of underactuated multibody systems". *Nonlinear Dynamics,* **67**, pp. 1539–1557.

[18] Seifried, R., and Eberhard, P., 2009. "Design of feed-forward control for underactuated multibody systems with kinematic redundancy". In Motion and Vibration Control: Selected Papers from MOVIC 2008, H. Ulbrich and L. Ginzinger, eds., Springer.

[19] Blajer, W., and Kolodziejczyk, K., 2004. "A geometric approach to solving problems of control constraints: Theory and a DAE framework theory and a DAE framework". *Multibody System Dynamics,* **11**, pp. 343–364.

[20] Blajer, W., and Kolodziejczyk, K., 2007. "Control of underactuated mechanical systems with servo-constraints". *Nonlinear Dynamics,* **50**, pp. 781–791.

[21] Seifried, R., and Blajer, W., 2013. "Analysis of servo-constraint problems for underactuated multibody systems". *Mechanical Sciences,* **4**, pp. 113–129.

[22] Bastos, G., Seifried, R., and Brüls, O., 2013. "Inverse dynamics of serial and parallel underactuated multibody systems using a DAE optimal control approach". *Multibody System Dynamics,* **30**, pp. 359–376.

[23] Morrison, D., Riley, J., and Zancarano, J., 1962. "Multiple shooting methods for two-point boundary value problems". *Communications of the ACM,* **5**, pp. 613–614.

[24] Keller, H., 1968. *Numerical Methods for Two-point Boundary-value Problems.* Blaisdell, Waltham, MA.

[25] Roberts, S., and Shipman, J., 1972. *Two-point boundary value problems: Shooting methods.* Elsevier, New-York.

[26] Chung, J., and Hulbert, G., 1993. "A time integration algorithm for structural dynamics with improved numerical dissipation: The generalized-α method". *ASME Journal of Applied Mechanics,* **60**, pp. 371–375.

[27] Newmark, N., 1959. "A method of computation for structural dynamics". *ASCE Journal of the Engineering Mechanics Division,* **85**, pp. 67–94.

[28] Arnold, M., and Brüls, O., 2007. "Convergence of the generalized-α scheme for constrained mechanical systems". *Multibody System Dynamics,* **18**(2), pp. 185–202.

[29] Arnold, M., Brüls, O., and Cardona, A., 2011. "Convergence analysis of generalized-α Lie group integrators for constrained systems". In Proceedings of Multibody Dynamics ECCOMAS Thematic Conference.

[30] Gear, C., Leimkuhler, B., and Gupta, G., 1985. "Automatic integration of Euler-Lagrange equations with constraints". *Journal of Computational and Applied Mathematics,* **12–13**, pp. 77–90.

[31] Brüls, O., E., L., Duysinx, P., and Eberhard, P., 2011. "Optimization of multibody systems and their structural components". In Multibody Dynamics: Computational Methods and Applications, Computational Methods in Applied Sciences, W. Blajer, J. Arczewski, K. Fraczek, and M. Wojtyra, eds., Vol. 23, Springer, pp. 49–68.

[32] Wasfy, T., and Noor, A., 2003. "Computational strategies for flexible multibody systems". *Applied Mechanics Review,* **56**(6), pp. 553–613.

[33] Bayo, E., and Ledesma, R., 1996. "Augmented lagrangian and mass-orthogonal projection methods for constrained multibody dynamics". *Nonlinear Dynamics,* **9**, pp. 113–130.

[34] Jay, L., and Negrut, D., 2007. "Extensions of the HHT-method to differential-algebraic equations in mechanics". *Electronic Transactions on Numerical Analysis,* **26**, pp. 190–208.

[35] Géradin, M., and Cardona, A., 2001. *Flexible Multibody Dynamics: A Finite Element Approach.* John Wiley & Sons, Chichester.

[36] Bastos, G., Seifried, R., and Brüls, O., 2011. "Inverse dynamics of underactuated multibody systems using a DAE optimal control approach". In Proceedings of the Multibody Dynamics ECCOMAS Conference.

[37] Wenger, P., and Chablat, D., 2009. "Kinematic analysis of a class of analytic planar 3-RPR parallel manipulators". In Computational Kinematics: Procedings of the 5th Internatinal Workshop on Computational Kinematics, pp. 43–50.